WFIRST-AFTA TECHNICAL REPORT
Doc#: WFIRST-STScI-TR1602
Rev: A
Date: April 12, 2016

SPACE TELESCOPE SCIENCE INSTITUTE

Saturation and Persistence Effects in the WFIRST Microlensing Observations

Kailash C. Sahu
Space Telescope Science Institute, Baltimore, MD

Abstract

In this report, we investigate the expected saturation and persistence effects in the WFIRST detector during the microlensing observations. We have calculated the expected intensity distribution of the detector pixels during the microlensing survey taking into account: (i) the number and luminosity distribution of the stars as observed by HST in the SWEEPS microlensing field, (ii) the expected shape of the PSF as generated by the WFIRST PSF simulator (webbPSF), and (iii) the expected countrates in the WFIRST observations as calculated by the Pandeia exposure time calculator. We combine this with a very basic persistence model where the persistence timescale (P) can be any value, but the affected pixels provide no useful data during this timescale. For P>>15min, if all the w149 observations are taken at a single dither position, 3.6% of the stars will be affected by persistence for the entire duration of the microlensing campaign, and the remaining 96.4% of the stars will be unaffected and hence have a 15-minute sampling interval. If one dither is applied in all the pointings, 7.2% of the stars will have sampling interval of 30 minutes, 92.8% of the stars will be unaffected and have the original sampling interval of 15 minutes. (The effects on the z087 observations are qualitatively similar.) It is known that larger numbers of dithers help in ensuring that photometry and astrometry are not minimally affected by bad pixels, or possible geometric solutions anomalies. However, for a given persistence timescale, the number of affected pixels N grows with the number of dithers until (no. of dithers * 15min) reaches P, after which the N remains constant. Conversely, for a given number of dither positions, the affected number of pixels increases with persistence timescale. We provide estimates of the fraction of stars with different sampling intervals for various persistence timescales and numbers of dithers.

1. Introduction: The WFIRST Microlensing Survey

A microlensing survey of the Galactic bulge is one of the principal observing programs of WFIRST, aimed at completing the planetary census begun by Kepler (WFIRST design reference mission, WFIRST SDT report, 2015). As per the current operations concept of the mission, the Microlensing survey will consist of observations carried out over a total of 6 (or, possibly 7) microlensing seasons of 72 days each. The full microlensing field will be covered through 10 WFIRST pointings. The observations will be repeated in a near-continuous fashion, so that the entire field will be observed every 15 minutes in the W149 filter, and once every 12 hours in the Z087 filter. The exposure times in these filters will be 52 sec in the W149 filter, and 290 sec in the Z087 filter.

2. Concerns for Possible Persistence Effects

The amplitude of photometric microlensing effects caused by earth-like planets is expected to be ~2% (Bennett and Rhie, 1988). Detecting such planets is the primary goal of the WFIRST observations, so the integration times chosen for the observations are such that the S/N achieved for most of the monitored stars would be large enough for detecting these planetary signals. The integration time of 52 sec in the F149 filter and 290sec in the Z087 filter would achieve a S/N>200 down to I~24, which would allow detection of such planetary signals. While the integration times employed here ensure sufficient S/N for the faint stars down to I~24, this also implies that some of the brighter stars would be saturated, possibly leading to persistence effects in the subsequent exposures, which would make it difficult to achieve the required precision in the affected pixels. Saturation of the brighter stars is thus a potentially serious concern, and it is important to quantify this effect. In this work, we have tried to quantify the number of stars and pixels expected to be saturated, taking the into account: (i) the number and luminosity distribution of the stars in the microlensing field, (ii) the PSF in the filters used, and (iii) the observational strategy as described above.

3. Stellar Density and Luminosity Function

The SWEEPS field observed by HST (Sahu et al. 2006), with an angular size ox 3.3x3.3 arcminutes, lies in a relatively higher stellar density region of the WFIRST microlensing field. The SWEEPS field is an ideal control field that can be used to investigate the persistence effects in the WFIRST detector for several reasons. First, this field is closer to the Galactic center where the microlensing optical depth is higher. As a result, this field will likely yield more microlensing events, so it is important to make sure that this region can be observed without any problems. Second, the SWEEPS field is fairly typical of the WFIRST microlensing field since the WFIRST field includes several low-extinction windows (such as the Baade's window and the Stanek window) where the stellar density and the brightness distributions are similar to the SWEEPS field. Furthermore, the SWEEPS field has been extensively observed by HST, which makes it possible to derive the stellar density distribution uncontaminated by blending effects. From our detailed study of the SWEEPS field, we have the full details of the spectral types and reddening measurements of the individual stars, which enables us to use this field to accurately estimate the expected count rates from WFIRST observations. The luminosity function as observed by ACS/HST in the I (F814W) band is shown in Fig. 1, which is also given in tabular form in Table 1.

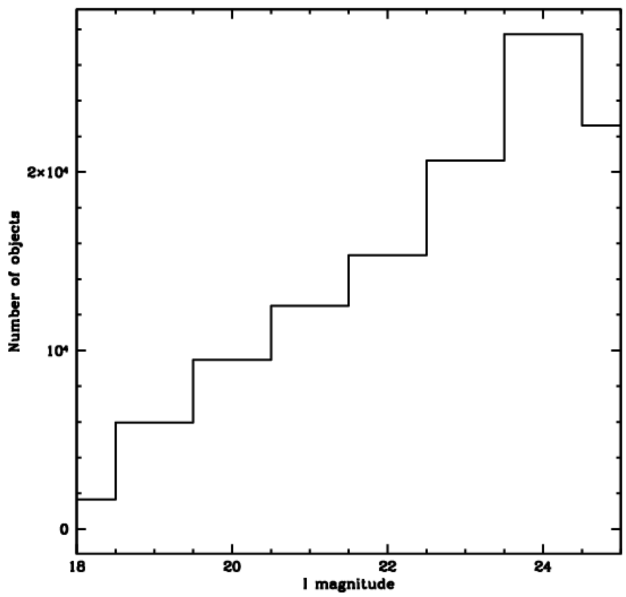

Fig. 1. The luminosity function as observed by ACS/HST in I (F814W) band is shown. Table 1 shows the actual number of stars as a function of the I-band magnitude. The turnover at I ~ 24 is due to incompleteness.

Table 1. Number and Luminosity Distribution of Stars in the SWEEPS field

I(F814W)	No. of stars in the SWEEPS field
15.00	30
15.50	36
16.00	73
16.50	116
17.00	211
17.50	470
18.00	918
18.50	3439
19.00	5906
19.50	7752
20.00	9508
20.50	11232
21.00	12319
21.50	13613
22.00	15155
22.50	17591
23.00	20054
23.50	23632
24.00	26637
24.50	26005
25.00	19954
25.50	10539

4. WFIRST Stellar PSF

We used the PSFs generated by the WFIRST PSF generator available through STScI WFIRST webbPSF simulator. We used a model stellar spectrum representing a spectral type corresponding to the average luminosity of the monitored stars. A representative PSF used in our calculations for the W149 filter is shown in Fig. 2.

Fig. 2. The shape of the PSF in the W149 filter as generated by the WFIRST PSF tool. We used the PSF generated by this tool in our calculations.

5. Expected Intensity Distribution in the Detector Pixels

We used the number and luminosity distribution of stars as observed in the SWEEPS field by HST to determine the expected intensity distribution in the WFIRST detectors. We used the Pandeia WFIRST exposure time calculator to estimate countrates in the two filters, using appropriate spectral types for the stars. Then, taking the shape of the PSF into account we calculated (i) the fraction of saturated stars, and (ii) the fraction of saturated pixels. It is important to notice the difference between these two since (i) some saturated stars affect more than 1 pixel, and (ii) some stars which are saturated in 52 seconds, can have good photometry if they are unsaturated in the first individual reads (assuming that the data from the individual reads are downloaded).

It is relatively easy to calculate the fraction of saturated stars. Taking the countrates into account, we find that a star with I=19.4 reaches saturation level of 36000 counts (D. Content, priv. comm.) in 52 seconds. If the data from individual reads are available, stars up to I~15 may be unsaturated. The corresponding fractions of saturated stars (for I< 19.4 and I<15) are 1.65 and 0.2%, respectively.

We then calculated the fraction of pixels which are expected to be affected by saturation. For this, we took the central 5x5 pixels of all the stars into account. This choice was made for the following two reasons. First, it was obvious that the intensity levels beyond 5x5 pixels in all but the very brightest few stars were too small to have any effect on the final result. Second, we realized that taking a much larger number of pixels for each star would make the number of pixels larger than the actual pixels in the detector.

The intensity distribution on different pixels not only depends on the shape of the PSF but also on where exactly the center of the light distribution falls on the pixel. To predict the intensity distribution in different pixels, we used two extreme scenarios. In the first scenario, we put all the stars in the center of a pixel. In the second scenario, we put all the stars in one corner of the pixels so that the intensity is equally distributed over 4 central pixels. The resultant intensity distribution over the pixels in these two scenarios are within 2% of each other. This is mainly due to the fact that for a star to affect 4 pixels at the same intensity level, the star needs to be brighter. The star in this case affects 4 pixels (rather than a single pixel), but there are fewer of such brighter stars since the number of stars decreases as the brightness increases. So we present here the results from the first scenario where the centers of all stars fall at the exact center of a pixel. We emphasize that the result changes by less than 2% if the stars are allowed to fall randomly on different pixels.

Figure 3 shows the result of this calculation where we plot the number of pixels at different count levels. An expanded view of the same figure between 0 to 2% of the pixels is shown separately at the bottom. If we assume that the stars with counts larger than 36,000 electrons show persistence effects, then 0.36% of the pixels are affected in each pointing. Assuming that (i) similar percentage of pixels are affected in each of the 10 pointings, (ii) there are no overlaps of the affected pixels, and (iii) the same stars fall exactly on the same pixels throughout the campaign (i.e. there is no dithering), the percentage of pixels which would be affected by persistence is 3.6 +/- 0.2%. We note that it takes 15 minutes to complete the observations of the entire microlensing field through 10 pointings. If the persistence lasts more than 15 minutes, these pixels will remain affected all the time. The remaining 96.4% of the monitored stars will be unaffected by persistence, and will have the sampling interval of ~15 minutes during the entire the microlensing campaign.

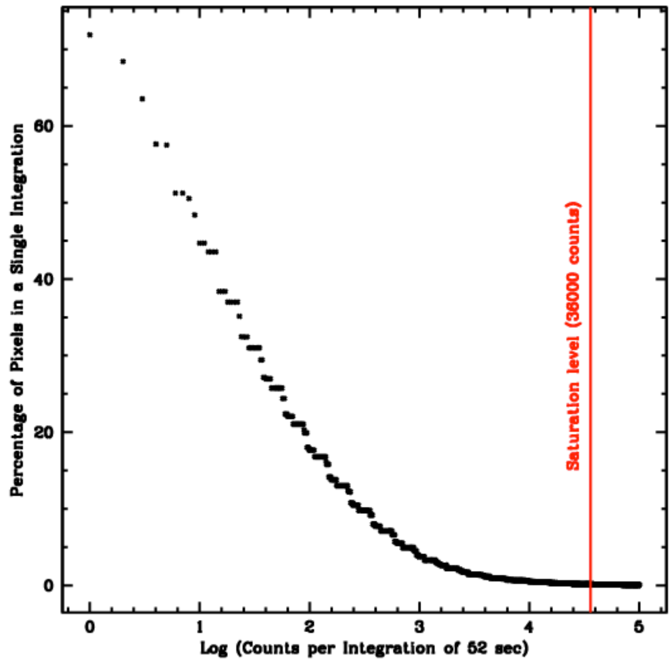

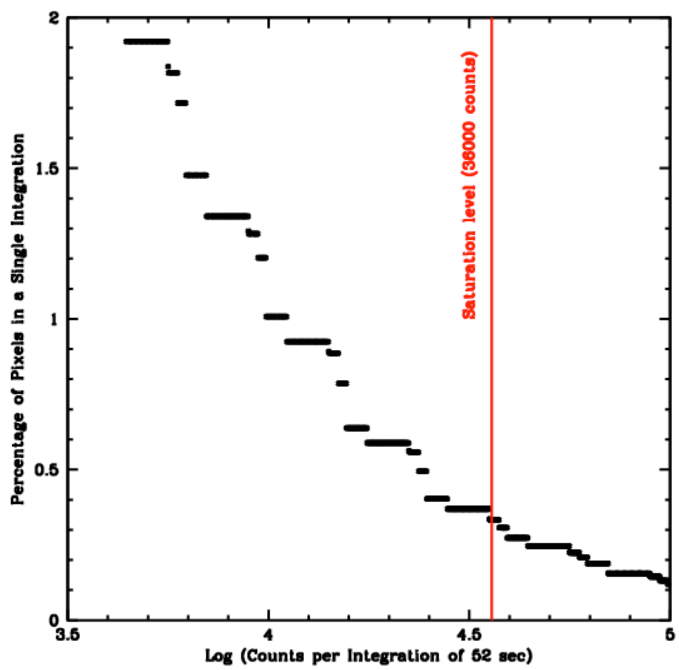

Fig. 3. The cumulative percentage of pixels above different count levels. Assuming a basic persistence model where stars with counts larger than 36,000 electrons show persistence effects (see text for more details), then 0.36% of the pixels are affected in each pointing. The top figure shows the entire range of the percentage of pixels, whereas the bottom figure shows an enlarged view of the percentage of pixels from 0 to 2%.

The actual persistence and saturation characteristics of the detector may be different depending on the final choice of the detector. The full characterization of the persistence characteristics of the detector is beyond the scope of the present study. But the percentage of pixels at different count levels reported here can be used with any persistence model.

6. Observations in the z087 Filter

The main purpose of the z087 observations is to look for any possible color terms in the light curve. This would require that the S/N in the z087 observations are similar to the S/N in the w149 observations. The integration times chosen for the z087 filter seem to indeed take this into account, so that the expected counts in both filters are similar. This also implies that the saturation characteristics in both filters will also be similar. So, to a first approximation, we can assume that the fraction of pixels at different count levels in the z087 observations are the same as in the w149 observations.

7. Observational Strategies with Dithering

W149 Observations: As described above, if there is no dithering at each pointing (i.e. if the stars at a given pointing fall exactly at the same locations in all the images), 3.6% of the stars will have no useful data, and all the remaining 96.4% of the stars will have 15 minute sampling interval. If one dither is applied to all pointings, 7.2% of the stars will have sampling interval of 30 min, 92.8% of the stars will be unaffected and have the original sampling interval of 15 minutes, and 0.2% will have no useful data. If we increase the number of dithers between observations, a larger number of stars will be affected by persistence at some stage. The full details are given in Table 2.

Z087 Observations: The situation is similar for the z087 filter. In this case, for persistence timescale $P \gg 12$ hr, if there is no dithering, 3.6% of the stars will have no useful data, and all the remaining 96.4% of the stars will have a 12-hour sampling interval. If one dither is applied to all pointings, 7.2% of the stars will have sampling interval of 24 hours, 92.8% of the stars will be unaffected and have the original sampling interval of 12 hours, and 0.2% will have no useful data.

TABLE 2. Fraction of stars/pixels affected by persistence

	No dither (n=1)**	**1 dither (n=2)**	**2 dithers (n=3)**	**25 dithers (n=26)**
Saturated stars in 52 sec (A)	1.65%	1.65%	1.65%	1.65%
Saturated stars in 1 sec (B) *	0.2%	0.2%	0.2%	0.2%
Pixels affected by persistence due to saturation (C)*** **C=C1*m where** **m= int(P/15min), if P<Q** **= n=Q/15min, if P≥Q**	3.6% (C1)	3.6%(m=1) to 7.2%(m≥2)	3.6%(m=1) to 10.8%(m≥3)	3.6%(m=1) to 93.6%(m≥26)
Stars with sampling interval (s*15) min **G=1-C1*(1+m-s), if m≥s** **G=1-B , if s>m**	96.4% to 99.8%	92.8% to 99.8%	89.2% to 99.8%	6.4% to 99.8%

Notes:

1. P=Persistence Timescale
2. Q=n*15min=Timescale for one full survey in all dither positions
3. The calculations here are for W149 observations for which the same field will be observed every 15 minutes. For z087, the calculations will be similar where “15 min” needs to be replaced with “12 hr”.
4. *We have assumed that the first read takes 1 sec, and that the first read data are downloaded. If not, B needs to be replaced with A throughout.
5. **No dither corresponds to observations at a single position, so n=1. Single dither corresponds to observations at 2 positions, so n=2, etc.
6. ***This corresponds to the worst-case scenario where the saturated pixels in different dithers do not overlap.

Future Work

In this work, the calculations of the percentage of pixels as a function of countrate were carried out as accurately as possible, taking into account the actual densities, luminosities and spectral characteristics of the stars in one of the WFIRST microlensing fields as observed by HST, and the model WFIRST PSFs. However, the persistence model used here is very basic, partly due to the fact that there is still considerable uncertainty on the actual persistence characteristics of the WFIRST detector. Future work should include more detailed persistence models. In particular, the persistence models should take into account the expected persistence as a function of countrate and time. Also, note that we have not addressed here the potential for post-observation calibration pipelines to (partially) correct any impacts of detector persistence.

Acknowledgements

This work was carried out under contract with the WFIRST Study Office at NASA Goddard Space Flight Center (GSFC), as part of the joint pre-formulation science center studies by the Space Telescope Science Institute (STScI) and the Infrared Processing and Analysis Center (IPAC). The author is grateful to Dave Content for initiating this study, and Jeff Kruk for encouragement and sharing the findings of alternate analyses. The author would like to thank Roeland van der Marel for useful comments.

References:

Bennett, D. and Rhie, 2002, ApJ, 574, 985
Sahu, K.C. et al. 2006, Nature, 443, 534
WFIRST SDT Report, 2015, Spergel, D. et al.